EUROPEAN JOURNAL OF CANCER 46 (2010) 2837–2848

available at www.sciencedirect.com

ScienceDirect

journal homepage: www.ejconline.com

Receptor tyrosine kinase and downstream signalling analysis in diffuse malignant peritoneal mesothelioma

Federica Perrone [a], *Genny Jocollè* [a], *Marzia Pennati* [b], *Marcello Deraco* [c], *Dario Baratti* [c], *Silvia Brich* [a], *Marta Orsenigo* [a], *Eva Tarantino* [a], *Cinzia De Marco* [b], *Claudia Bertan* [a], *Antonello Cabras* [a], *Rossella Bertulli* [d], *Marco Alessandro Pierotti* [e], *Nadia Zaffaroni* [b], *Silvana Pilotti* [a,*]

[a] *Experimental Molecular Pathology, Department of Pathology, Fondazione IRCCS Istituto Nazionale dei Tumori, Via G. Venezian 1, 20133 Milano, Italy*

[b] *Department of Experimental Oncology and Molecular Medicine, Fondazione IRCCS Istituto Nazionale dei Tumori, Via G. Venezian 1, 20133 Milano, Italy*

[c] *Department of Peritoneal Tumor, Fondazione IRCCS Istituto Nazionale dei Tumori, Via G. Venezian 1, 20133 Milano, Italy*

[d] *Adult Sarcoma Unit, Fondazione IRCCS Istituto Nazionale dei Tumori, Via G. Venezian 1, 20133 Milano, Italy*

[e] *Scientific Management, Fondazione IRCCS Istituto Nazionale dei Tumori, Via G. Venezian 1, 20133 Milano, Italy*

ARTICLE INFO

Article history:
Received 8 March 2010
Received in revised form 22 June 2010
Accepted 24 June 2010
Available online 6 August 2010

Keywords:
Diffuse malignant peritoneal mesothelioma
EGFR
PDGFRB
p16
mTOR

ABSTRACT

Our aim was to assess the activation profile of EGFR, PDGFRB and PDGFRA receptor tyrosine kinases (RTK) and their downstream effectors in a series of cryopreserved diffuse malignant peritoneal mesothelioma (DMPM) surgical specimens to discover the targets for drug inhibition. We also made a complementary analysis of the cytotoxic effects of some kinase inhibitors on the proliferation of the human peritoneal mesothelioma STO cell line.

We found the expression/phosphorylation of EGFR and PDGFRB in most of the tumours, and PDGFRA activation in half. The expression of the cognate ligands TGF-α, PDGFB and PDGFA in the absence of RTK mutation and amplification suggested the presence of an autocrine/paracrine loop. There was also evidence of EGFR and PDGFRB co-activation. RTK downstream signalling analysis demonstrated the activation/expression of ERK1/2, AKT and mTOR, together with S6 and 4EBP1, in almost all the DMPMs. No *KRAS/BRAF* mutations, *PI3KCA* mutations/amplifications or *PTEN* inactivation were observed. Real-time polymerase chain reaction revealed the decreased expression of TSC1 c-DNA in half of the tumours. *In vitro* cytotoxicity studies showed the STO cell line to be resistant to gefitinib and sensitive to sequential treatment with RAD001 and sorafenib; these findings were consistent with the presence of the *KRAS* mutation G12D in these cells although it was not detectable in the original tumour.

Our results highlight the ligand-dependent activation and co-activation of EGFR and PDGFRB, as well as a connection between these activated RTKs and the downstream mTOR pathway, thus supporting the role of combined treatment with RTK and mTOR inhibitors in DMPM.

* *Corresponding author:* Tel.: +39 02 2390 2293; fax: +39 02 2390 2877.
E-mail address: silvana.pilotti@istitutotumori.mi.it (S. Pilotti).

0959-8049/$ - see front matter © 2010 Elsevier Ltd. All rights reserved.
doi:10.1016/j.ejca.2010.06.130

1. Introduction

Diffuse malignant peritoneal mesothelioma (DMPM) is a rare tumour that accounts for 10–20% of all forms of malignant mesothelioma. It was once regarded as a rapidly lethal disease but, over the last few years, survival has remarkably improved (up to 5 years) as a result of the introduction of intensive loco-regional treatment including cytoreductive surgery together with perioperative intraperitoneal chemotherapy in the form of intraperitoneal hyperthermic chemotherapy (HIPEC) +/- early postoperative intraperitoneal chemotherapy.[1,2] However, for those patients not amenable to curative treatment, due to advanced disease stage or deterioration of clinical conditions, prognosis remains poor and systemic treatment is still unsatisfactory.[3] Furthermore, approximately 40–60% of patients recurs, but optimal management of recurrent or progressive DMPM has never been standardised.[4]

Clearly, there is a need to explore new therapies in management of this tumour. One of these is to try to improve our understanding of DMPM molecular and cytogenetic biology, which might make it possible to identify specific new drugs and biomarkers useful for selecting the patients who could benefit from them.

Little is known about DMPM biology, although the prognostic impact of a few biomarkers has been investigated, mainly by means of immunohistochemistry and fluorescence *in situ* hybridisation. It has been reported that reduced or no p16 protein expression is a frequent alteration in DMPMs and pleural mesotheliomas[5,6] but, although homozygous deletion of the 9p21 locus harbouring the $p16^{INK4a}$ gene significantly correlates with pleural mesothelioma (67–100%), only a small (25%) fraction of DMPMs shows 9p21 deletion.[6,7] On the contrary, EGFR overexpression seems to be significantly more frequent in DMPMs than in pleural mesotheliomas (92% *versus* 33%, $p = 0.0004$),[5,8,9] and both pleural and peritoneal mesotheliomas are negative for c-Kit protein expression.[9,10]

The prognostic significance of loss of p16 expression is controversial,[3,11] while overexpression of EGFR,[8] matrix metalloprotease-2 (MMP-2) and MMP-9 is described in DMPMs[5] did not correlate with prognosis. On the contrary, it has recently been reported that telomerase activity is expressed in the majority of DMPMs and that it negatively affects the clinical outcome of patients undergoing cytoreductive surgery and hyperthermic i.p. chemotherapy.[12]

Potentially targetable biomarkers are indicated by the overexpression of cytoprotective factors (such as survivin and the other members of the family of apoptosis protein inhibitors) in most DMPMs.[13] For example, it has been found that siRNA-mediated survivin knockdown in DMPM cells enhances both spontaneous and cisplatin/doxorubicin-induced apoptosis, thus supporting the notion that survivin antagonists (such as YM-155, which is currently being tested in phase I and II trials) may provide new approaches to the treatment of DMPMs.[14] Moreover, microarray analysis, revealing a distinct molecular signature between epithelial and biphasic DMPM, indicated the ubiquitin–proteasome pathway as a potential therapeutic target in biphasic tumours as it was found upregulated.[15]

Despite the development and present availability of a wide spectrum of drugs targeting receptor tyrosine kinases (RTKs), little is known concerning their status and downstream effectors in DMPMs. There are no published data concerning PDGFRB and PDGFRA expression in DMPMs, whereas both,[16] and particularly PDGFRB,[17,18] are expressed in pleural mesotheliomas, although neither plays a diagnostic role nor affects patient outcome. Finally, a recent mutational analysis of exons 18–24 spanning the entire EGFR tyrosine kinase domain found EGFR mutations in 31% of the 29 DMPMs investigated.[19]

Taking advantage of the availability of a series of DMPM undergoing cytoreductive surgery and subsequent HIPEC, we assessed the deregulation of RTKs (EGFR, PDGFRB and PDGFRA) and their downstream effectors in an attempt to identify the targets susceptible to drug inhibition. This analysis was complemented by a study of the effects of some kinase inhibitors on the proliferation of a human DMPM cell line.

2. Materials and methods

2.1. Samples and patients

We analysed DMPM specimens taken from 20 patients who were treated by cytoreductive surgery and subsequent HIPEC at Fondazione IRCCS Istituto Nazionale dei Tumori between 2007 and 2008. Their ages and gender are listed in Table 1. Seventeen DMPMs were histologically classified as epitheliod, one biphasic, one sarcomatoid and one papillary. All the diagnoses were confirmed by immunophenotyping, including immunoreactivity for calretinin (Ventana, pre-diluted), keratin 5 and 6 (clone D5/I6B4, Zymed, diluted 1:50), podoplanin (AngiBio, diluted 1:400) and Wilms' tumour 1 proteins (polyclonal antibody, Santa Cruz, diluted 1:200), and a claudin 4 null immunophenotype (clone 3E2C1, Zymed, diluted 1:25).

The biochemical analyses were performed on frozen surgical samples obtained directly from the surgeon during surgery, whereas the other analyses were based on formalin-fixed paraffin embedded (FFPE) material. Morphologically normal tissue was also obtained from non-tumoural FFPE specimens surrounding the DMPM.

Our institution is the Italian reference centre for DMPM, affording an adequate recruitment of patients affected by such rare malignancy and uniformity of treatment protocol.

2.2. Analysis of frozen material

2.2.1. Phosphorylation of RTK array

The expression of phosphorylated growth factor RTKs was detected by means of the phosphor proteome profiler Array kit (R&D Systems) as described in the manufacturer's protocol using 2 mg of protein lysate per array extracted as previously described.[20]

2.2.2. Immunoprecipitation and Western blotting

The experimental conditions for EGFR, PDGFRA and PDGFRB immunoprecipitation and subsequent Western blotting (WB) have been previously described.[21,22] PTEN, AKT, ERK1/2,

Table 1 – RTK analysis.

Case	Sex/age	Hystotype	EGFR			PDGFRB			PDGFRA			Ligands			p16	
			WB expr	WB phos	IHC	WB expr	WB phos	IHC	WB expr	WB phos	IHC	TGF-α	PDGFB	PDGFA	IHC	FISH
1	F/37	epitheliod	++	–	neg	+	–	pos	++	+	pos	+	+	+	neg	D
2	M/59	epitheliod	++	+++	inter	++	+	pos	+	–	pos	+	+	+	neg	D
3	M/28	sarcomatoid	+	+	neg	+++	+	pos	+	–	pos	+	+	+	pos	D
4	F/50	biphasic	++	+	neg	+++	++	neg	++	++	pos	+	+	+	neg	D
5	F/44	epitheliod	+	+	high	+++	–	pos	++	–	pos	+	+	+	neg	HD
6	M/65	epitheliod	++	+	high	+++	–	neg	+	–	pos	+	+	+	neg	M
7	M/65	epitheliod	++	+++	inter	++	+	pos	++	+	pos	+	+	+	neg	D
8	F/51	epitheliod	++	+++	low	+	–	pos	++	–	low	+	+	+	pos	ne
9	M/71	epitheliod	+	+	neg	++	+	pos	++	+	pos	+	+	+	pos	D
10[a]	F/66	epitheliod	++	+++	high	++	+	pos	++	+	low	+	+	+	pos	LP
11	F/77	epitheliod	++	+++	high	++	+	pos	++	+	pos	+	+	+	neg	D
12	F/76	epitheliod	++	+	high	–	–	pos	+	–	pos	+	+	+	pos	D
13	F/52	papillary	+++	++	high	++	+	neg	–	–	neg	+	+	+	pos	D
14	F/55	epitheliod	++	++	low	+++	+++	pos	–	–	neg	+	+	+	pos	D
15	F/66	epitheliod	+++	+++	high	+	+++	pos	++	++	pos	+	+	+	neg	D
16	F/40	epitheliod	++	+	inter	+++	++	pos	+	–	pos	+	+	+	neg	D
17	M/67	epitheliod	++	++	high	++	+++	pos	+	–	pos	+	+	+	neg	ne
18	F/68	epitheliod	+	++	high	+	+	neg	++	+	pos	+	+	+	neg	LP
19	M/69	epitheliod	++	++	high	++	++	low	–	–	pos	+	+	+	neg	D
20	M/54	epitheliod	++	++	inter	++	++	pos	++	++	pos	+	+	+	pos	D

M, male; F, female; +, positive; –, negative; neg, negative; pos, positive; inter, intermediate.
D, disomy; HD, homozygous deletion; M, monosomy; LP, low polysomy.
WB expr, Western blot expression; WB phos, Western blot phosphorylation; IHC, immunohistochemistry; FISH, fluorescence in situ hybridization; RTK, receptor tyrosin kinase.
a Case carrying low polysomy of chromosomes 7, 5 and 4.

mTOR and S6 expression/activation was analysed by means of direct WB using 20 μg of total protein, previously described antibodies and dilutions.[21,23]

To detect the possible activation of 4EBP1, WB experiments were performed using the anti-phopsho-4EBP1 antibody (9455S, Cell Signaling, diluted 1:1000). Subsequently, the filter was stripped and incubated with anti-4EBP1 antibody (9644, Cell Signaling, diluted 1:1000) to assess protein expression.

The positive controls of expression/phosphorylation were the NIH3T3 cell line (American Type Culture Collection, Manassas, VA) for PDGFRA; the Cal27 cell line for EGFR; the 2N5A cell line (derived from the NIH3T3 cell line and expressing the COL1-PDGFB fusion characterising dermatofibrosarcoma protuberans, kindly provided by Dr. A. Greco, Experimental Oncology Department, Fondazione IRCCS Istituto Nazionale dei Tumori, Milan, Italy) for PDGFRB, AKT and ERK1-ERK2; and the A431 cell line for PTEN, mTOR, S6 and 4EBP1.

2.3. *Analysis of FFPE material*

2.3.1. *Immunohistochemistry (IHC)*

The IHC analyses were made using 2 μm cut FFPE tumoural sections.[24] EGFR was immunostained using the EGFR-DAKO kit, and the level of staining was scored as high, intermediate and low as previously described.[24] PDGFRA and PDGFRB were analysed using antibodies against PDGFRA (clone sc338, Santa Cruz Biotechnology, CA; diluted 1:200) and PDGFRB (clone sc339, Santa Cruz Biotechnology, CA; diluted 1:100), and previously described protocols and positive controls.[21] p16 was analysed using a CINtec Histologic Kit (MTM Laboratories AG, Heidelberg, Germany) following the instruction for use. Positivity was defined as >50% of cells showing moderate/strong cytoplasmic immunolabelling.

2.3.2. *Real-time quantitative polymerase chain reaction (PCR)*

After RNA extraction and retrotranscription,[22] TGF-α, PDGFB and PDGFA c-DNAs were detected by means of real-time PCR using a TaqMan assay (ABIPRISM 5700 PCR Sequence Detection Systems, Applied Biosystems Foster City, CA, USA) as previously described,[21,25] and PI3K, TSC1 and TSC2 c-DNAs were relatively quantified by means of real-time quantitative PCR using the $2^{-\Delta\Delta Ct}$ method.[26] In each case, the calibrator sample was the corresponding non-tumoural tissue.

2.3.3. *Mutational analysis*

After DNA extraction performed through microdissection,[27] we analysed mutations in EGFR (exons 18–21), PDGFRB (exons 12, 14 and 18), PDGFRA (exons 12, 14 and 18), PTEN (exons 5–8), PI3KCA (exons 9 and 20), KRAS (exons 1) and BRAF (exons 11 and 15) as previously described.[21]

2.3.4. *Fluorescence in situ* hybridisation (FISH)

FISH was used to analyse EGFR, PDGFRA, PDGFRB, PTEN, PI3KCA and $p16^{INK4a}$ genes in representative areas of 2 μm tumoural sections selected under microscopic control as previously described.[21,24]

2.4. In vitro studies

2.4.1. Cell line and drugs

The mycoplasma-free STO human peritoneal mesothelioma cell line established in our laboratory[13] was grown as a monolayer in DMEM F-12 medium (Lonza Milano s.r.l, Treviglio, Italy) supplemented with 10% foetal bovine serum in a 37 °C humidified 5% CO_2 incubator. The cells were characterised for EGFR, PDGFRA, PDGFRB, ERK1/2, AKT, mTOR, S6 and 4EBP1 expression/activation by means of immunoprecipitation and Western blotting experiments, and *KRAS, BRAF, PI3KCA* and *PTEN* mutations under the conditions described above.

RAD001 (Everolimus) was purchased from Sigma Aldrich (St. Louis, MO, USA), gefitinib from Astra Zeneca (London, UK) and sorafenib from Bayer (Milan, Italy). RAD001 and sorafenib were dissolved in dimethylsulphoxide (DMSO) and gefitinib in ethanol (EtOH), stored at 20 °C, and then diluted in complete culture medium immediately before use.

2.4.2. SRB cytotoxicity assay

After being harvested during the logarithmic growth phase, 2×10^3 cells were plated in 96-well flat-bottomed microtitre plates (EuroClone, Milan, Italy) for 48 h and treated with increasing concentrations of RAD001, gefitinib or sorafenib individually administered for 72 h, or with RAD001 for 24 h followed by sorafenib for 48 h. The control cells received vehicle alone (DMSO or EtOH). At the end of drug exposure, cytotoxicity was determined by means of a sulphorhodamine B (SRB) assay as previously described.[28] Briefly, the cells were fixed and stained with SRB solution for 30 min, after which the plates were washed to remove any unbound stain, air-dried, and the bound stain was dissolved by 10 mM Tris base. Optical density was read at 550 nm on a microplate reader, with the results being expressed as the values in the treated samples in comparison with controls. Dose–response curves were created, and IC_{50} values (i.e. the concentrations capable of inhibiting cell growth by 50%) were determined graphically from the curves for each drug.

The method described by Chou and Talalay[29] was used to establish the nature of the interaction between the cytotoxic effects of RAD001 and sorafenib, which were always combined at a fixed RAD001:sorafenib concentration ratio of 1:25. The interaction was quantified by determining a combination index (CI): CI values of <1 or >1, respectively, indicate synergy or antagonism; a CI value of 1 indicates an additive effect.

2.4.3. Apoptosis analysis

After drug treatment, the adherent and detached cells were pooled and stained with a solution containing 50 mg/ml of propidium iodide, 50 mg/ml of RNase and 0.05% Nonidet P40 in PBS for 30 min at 4 °C. They were then spotted onto slides and assessed for typical apoptotic nuclear morphology (nuclear shrinkage, condensation and fragmentation) by means of fluorescence microscopy with appropriate filter combinations. The number of apoptotic cells was determined by two independent observers who scored at least 500 cells in each sample. The APOPCYTO/caspase-3 assay kit (Medical & Biological Laboratories, Naka-ku Nagoya, Japan) was used as previously described to measure the catalytic activity of caspase-3 in the same samples as the ability to cleave the specific substrate N-acetyl-Asp-Glu-Val-Asp-AMC (DEVD-AMC).[13]

2.5. Statistical analysis

The data were analysed using a two-tailed Student's *t*-test. *P* values of <0.05 were considered statistically significant.

3. Results

3.1. RTK analysis

3.1.1. RTK expression/activation

3.1.1.1. Biochemical analysis. Frozen surgical specimes of the 20 DMPMs were investigated for EGFR, PDGFRB and PDGFRA expression and phosphorylation status by means of immunoprecipitation and WB (Table 1). Almost all the cases showed EGFR and PDGFRB expression; EGFR and PDGFRB phosphorylation levels similar to or higher than those observed in the controls were found in, respectively, 90% and 75%. PDGFRA expression was found in 17 cases (85%), only 45% of which showed low levels of receptor activation (Fig. 1A shows some representative cases).

3.1.1.2. IHC. Immunohistochemical analysis revealed EGFR expression in 16 cases (80%), 14 of which had a high or intermediate score (Table 1). PDGFRB cytoplasmic immunoreactivity was also found in 80% of the cases.

PDGFRA immunostaining revealed the cytoplasmic receptor expression in 18 cases (90%), but two cases were only weakly positive (Table 1).

The inconsistent results observed in cases #1, #3, #4, #6, #9, #12, #13 and #18 may have been due to the different sensitivity of the antibodies used for the immunohistochemistry and biochemical analyses.

3.1.1.3. Phospho RTK antibody arrays. The expression of different phosphorylated RTKs was evaluated in four of the frozen DMPMs using the phospho-proteome profiler array kit. In line with the immunoprecipitation western blot findings, all of the tumours had a similar activation profile, characterised by high levels of EGFR activation, high/moderate levels PDGFRB activation, and very low or no PDGFRA activation (Fig. 1B); in some cases, M-CSF-R, IGF-1R and insulin receptors were also activated.

3.2. RTK activation mechanisms

3.2.1. Ligand expression

The expression of the cognate ligands TGF-α, PDGFB and PDGFA was investigated by means of real-time PCR, which showed that all the cases expressed c-DNAs encoding the three ligands (Table 1). Fig. 1C shows some representative cases.

3.2.2. EGFR–PDGFRB heterodimerisation

Evidence of the presence of EGFR–PDGFRB heterodimers was obtained in all six DMPMs analysed in co-immunoprecipitation experiments. After protein extract immunoprecipitation with EGFR antibody, WB experiments using PDGFRB revealed

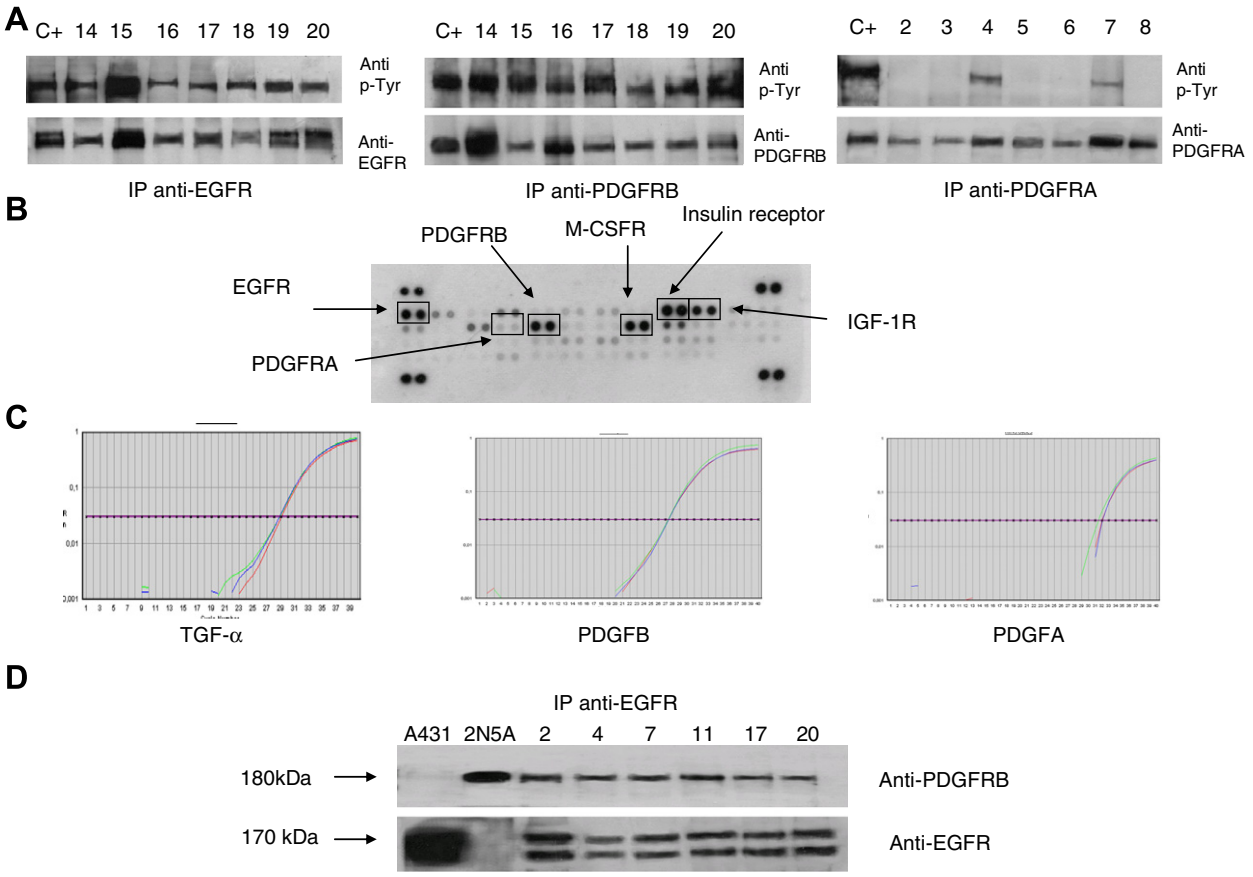

Fig. 1 – RTK analyses. (A) EGFR, PDGFRB and PDGFRA IP and WB experiments. The bands correspond to the activated (upper rectangles) and expressed receptors (lower rectangles) in the tumour samples. (B) Expression profiles of different phosphor RTKs in DMPM. The spots in the rectangles represent the activated EGFR, PDGFRB, M-CSFR, insulin and IGF-1R receptors; PDGFRA was inactivated. The double strongly labelled spots at the four corners represent the positive controls. (C) Ligand expression. Real-time PCR experiments showed the expression of TGF-α, PDGFB and PDGFA c-DNAs. (D) Evidence of EGFR-PDGFRB heterodimerisation. After EGFR IP, WB experiments using anti-PDGFRB antibody revealed a 180 kDa band corresponding to PDGFRB. Subsequent incubation with EGFR antibody revealed a band of 170 kDa in all the analysed samples. The 2N5A and A431cell lines were respectively used as positive controls for PDGFRB and EGFR. Abbreviations: IP, immunoprecipitation; WB, Western blotting; C+, positive control.

the specific bands corresponding to the receptor (Fig. 1D); further WB using EGFR antibody confirmed the EGFR expression in all cases.

3.2.3. *Mutational analysis*

Automatic sequencing of the genomic DNA encoding for the tyrosine kinase domain of EGFR (exons 18–21), the juxtamembrane region (exon 12), and the tyrosine kinase domain (exons 14–18) of the PDGFRB and PDGFRA genes did not reveal mutations.

3.2.4. *FISH analysis*

As an increased RTK gene copy number (through gene amplification or polysomy) can sustain receptor activation, we assessed RTK status by means of cytogenetic analysis, but none of the cases showed any gene amplification. Most of the cases had a disomic pattern; only one (#10) showed low polysomy of the three chromosomes containing the receptors.

Taken together, the expression of the ligands coupled with RTK heterodimerisation in the absence of any RTK gene mutation or gain in copy number suggests an autocrine/paracrine activation loop.

3.3. *p16 analysis*

This analysis was made in order to verify the published data. Immunohistochemical analysis revealed a p16 null immunophenotype in 12 of the 20 MPMs (60%), two of which carried a homozygous deletion of the 9p21 locus containing $p16^{INK4a}$ or showed monosomy of chromosome 9 as assessed by FISH. Our results confirmed both the previously reported frequent absence of p16 expression and the rare deletion of the p16 gene. Other molecular mechanisms sustaining the loss of p16 expression have not yet been clarified.

3.4. *RTK downstream target analysis*

3.4.1. *AKT/PI3K pathway*

3.4.1.1. AKT analysis. AKT expression and activation were investigated by means of direct WB experiments. All the

Table 2 – RTK downstream analysis.

Case	AKT		PI3KCA		PTEN			ERK		KRAS	BRAF	mTOR		TSC1	TSC2	S6		4EBP1	
	WB expr	WB phos	mut	FISH	mut	FISH	WB expr	WB expr	WB phos	mut	mut	WBexpr	WBphos	2-AACt	2-AACt	WB expr	WB phos	WB expr	WB phos
1	++	++	wt	D	wt	ne	++	++	++	wt	wt	++	++			++++	++++	+++	+
2	++	+++	wt	D	wt	D	+	++	+++	wt	wt	+	+			+	–	+++	++
3	++	++	wt	LP	wt	D	++	++	+++	wt	wt	++	+	10.41	21.55	+++	++	+++	++
4	++	++	wt	D	wt	D	++	++	+++	wt	wt	+	++			++	+	+++	+++
5	++	++	wt	LP	wt	D	+	+	++++	wt	wt	+	+			+	–	+++	++
6	++	+	wt	D	wt	D	+	++	+	wt	wt	+++	+++			+++	+++	+++	+++
7	++	++	wt	LP	wt	D	+	+	++++	wt	wt	+	++	0.48	1.61	++	++	++	+
8	++	++	wt	D	wt	D	+	++	++++	wt	wt	+	++			+	+	+	–
9	++	++	wt	D	wt	D	+	++	++++	wt	wt	++	++	4.23	7.83	+	++	++	++
10[a]	++	++	wt	LP	wt	LP	++	++	++++	wt	wt	+++	+++	4.92	9.80	+++	+++	+++	++
11	++	++	wt	D	wt	D	++	++	++++	wt	wt	++	++	1.19	3.40	+++	+++	+++	+++
12	++	+	wt	D	wt	D	++	++	+	wt	wt	–	–			+	+	++	++
13	++	++	wt	D	wt	D	+	++	+++	wt	wt	++	++	0.50	2.40	+	+	++	++
14	++	++	wt	D	wt	D	+	++	+++	wt	wt	++	++	0.65	1.42	–	–	++	++
15	++	++	wt	D	wt	D	++	++	++	wt	wt	++	++	0.85	4.17	+++	+++	++	++
16	++	+	wt	D	wt	D	+	++	++	wt	wt	++	++	2.14	7.70	+	+	+	+
17	++	+	wt	LP	wt	D	+	++	++	wt	wt	++	++	0.81	5.29	++	+	++	++
18	++	++	wt	D	wt	D	+	++	++	wt	wt	++	++	0.41	0.24	++	++	++	++
19	++	+	wt	D	wt	D	+	++	+++	wt	wt	++	++	0.43	29.04	++	++	++	++
20	++	+	wt	D	wt	D	+	+	+++	wt	wt	++	++	1.20	3.43	++	++	+	+

WB expr, Western blot expression; WB phos, Western blot phosphorylation; FISH, fluorescence in situ hybridization; wt, wild-type; mut, mutation

a Case carrying low polysomy of chromosomes 7, 5 and 4.

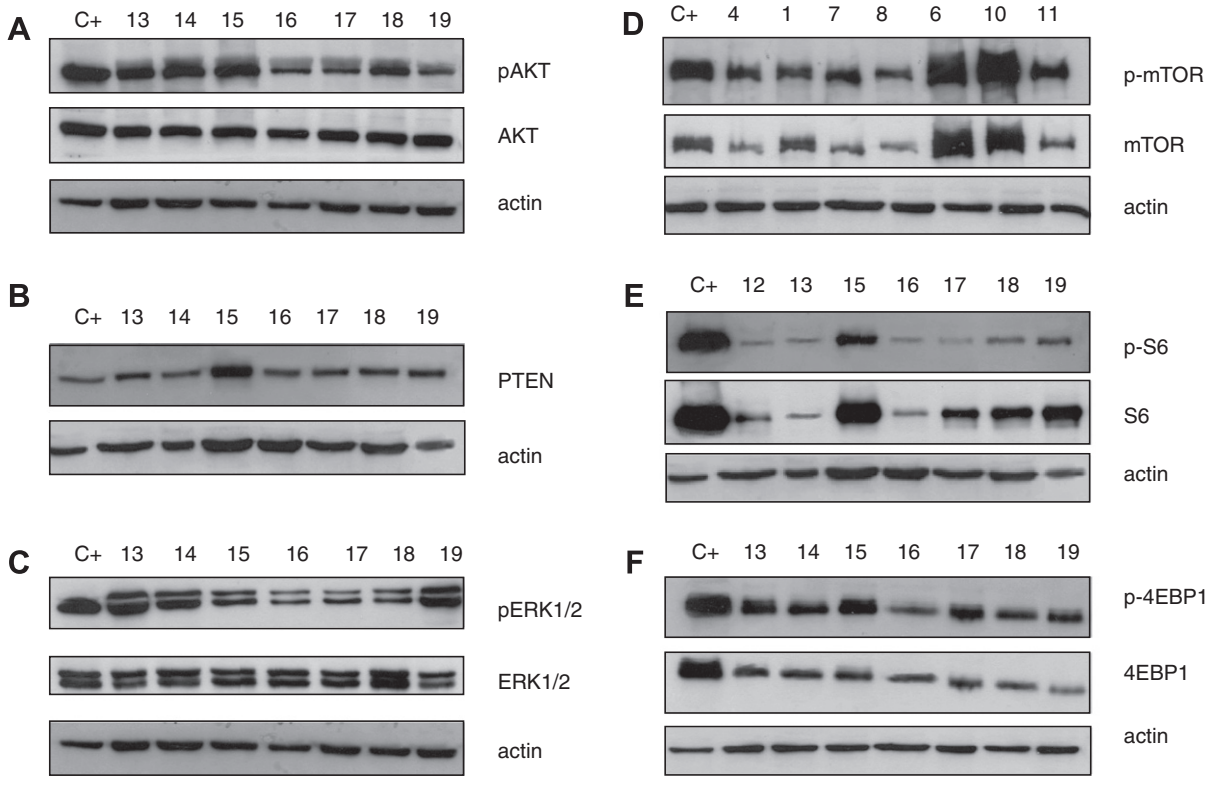

Fig. 2 – RTK downstream effector biochemical analysis. In the case of AKT, ERK1/2, mTOR, S6 and 4EBP1, the upper rectangle indicates the phosphorylated (*p*) form of the effector obtained by means of WB experiments using the specific phospho-antibody, whereas the lower rectangle represents the expressed forms. WB experiments using an anti-PTEN antibody revealed protein expression in all cases. Abbreviation: C+, positive control.

samples showed AKT expression and phosphorylation (Table 2); Fig. 2A shows some representative cases.

3.4.1.2. PI3KCA analysis. In order to assess possible activating mutations, exons 9 and 20 of the *PI3KCA* gene were sequenced, but no mutations were found in any of the cases (Table 2).

FISH analysis revealed a low polysomy of chromosome 3 containing the PI3KCA gene in five cases (25%); the others had a disomic pattern (Table 2).

In order to verify whether the low polysomy of chromosome 3 reflected increased PI3KCA transcript expression, we assessed the relative PI3KCA c-DNA levels by means of real-time PCR in 15 DMPMs using the ΔCt method. All but four tumours showed PI3KCA expression, without any difference in ΔCt between those showing low polysomy or disomy of chromosome 3, thus suggesting that the gene status does not influence transcript expression (data not shown). Moreover, PI3KCA c-DNA levels were undetectable in the non-tumoural tissue (despite the expression of the housekeeping gene), thus suggesting that the DMPMs expressed more PI3KCA c-DNA (Table 2).

3.4.1.3. PTEN analysis. Mutational analysis of the *PTEN* gene (exons 5–9) did not reveal any mutations (Table 2).

In order to assess potential *PTEN* gene loss, FISH analysis was successful in 19 of the 20 DMPMs, all but one of which had a normal disomic pattern (Table 2); the other carried low polysomy of chromosome 10. Consistently, all the DMPMs homogeneously expressed PTEN protein in WB experiments (Fig. 2B).

3.5. *ERK pathway*

3.5.1. *RAS and BRAF analysis*

The samples were investigated for KRAS and BRAF activating mutations, but none were found (Table 2).

3.5.2. *ERK1/2 analysis*

ERK1 (band of 42 kDa) and ERK2 (band of 44 kDa) were intensely expressed and activated in all the samples (Table 2). Fig. 2C shows some representative cases.

3.6. *mTOR pathway*

3.6.1. *mTOR analysis*

WB revealed mTOR expression and phosphorylation in all but one case (Table 2) at signal levels that were mainly similar to those observed in the positive control. Fig. 2D shows some representative cases.

3.6.2. *S6 and 4EBP1*

The expression and activation of the two main mTOR downstream effectors, S6 (Fig. 2E) and 4EBP1 (Fig. 2F) were biochemically assessed (Fig. 2). Both were frequently expressed (S6 95%, and 4EBP1 100%), and showed significant phosphorylation (S6 85%, and 4EBP1 95%) (Table 2).

3.6.3. *Quantitative analysis of TSC1 and TSC2*

As the down-regulation of the TSC1 and TSC2 tumour suppressor genes, which act as negative regulators of mTOR, could favour mTOR activation, we relatively quantified their c-DNAs by means of real-time quantitative PCR in matched tumour and normal tissues using the $2^{-\Delta\Delta Ct}$ method. The DMPM values are given as fold-expression levels in comparison with the corresponding non-tumoural tissue used as the calibrator sample for each tumour.

TSC1 c-DNA expression was less than in the corresponding non-tumoural tissue in seven cases (54%) (Table 2), with a median $2^{-\Delta\Delta Ct}$ value of 0.59, whereas only one case (#34) showed less TSC2 c-DNA expression with a $2^{-\Delta\Delta Ct}$ value of 0.24.

3.7. *In vitro studies*

The molecular pathology results indicated that the activation of downstream RTK signalling in the DMPM specimens is mediated by the activation of EGFR and PDGFRB RTKs, thus suggesting a rationale for using RTK and mTOR inhibitors (alone and in combination) to treat the disease. In order to test this hypothesis, we evaluated the antiproliferative effects of the EGFR inhibitor gefitinib, the mTOR inhibitor RAD001 and multikinase inhibitor sorafenib (which targets PDGFRB, VEGFR-2 and VEGFR-3, the serine-threonine kinase Raf)[30] in the STO human peritoneal mesothelioma cell line.

We first biochemically analysed the RTK activation profile of the STO cell line and observed EGFR expression and activation in the absence of any receptor mutation, whereas neither PDGFRB nor PDGFRA was expressed or activated. Analysis of downstream RTK signalling revealed ERK1/2, AKT, mTOR, S6 and 4EBP1 expression/phosphorylation (data not shown).

In a preliminary set of experiments, the cells were treated with increasing concentrations of the individual drugs in a 72-h SRB assay and a concentration-dependent reduction in cell survival was observed in all cases (Fig. 3). However, the antiproliferative effect of gefitinib was only appreciable at very high drug concentrations, as indicated by its IC_{50} of 40.1 ± 1.3 μM. Given the resistance of the STO cells to gefitinib, we performed a mutational analysis of the downstream RTK effectors, which revealed *KRAS* mutation (G12D) and the absence of *BRAF*, *PI3KCA* and PTEN mutations. It is worth noting that the DMPM specimen from which the STO cell line derives was KRAS wild-type, which suggests the possible in-culture selection of a subpopulation of *KRAS* mutated cells that were already present but undetectable in the original tumour.

Interestingly, the STO cells seemed to be highly sensitive to sorafenib, as suggested by the much lower IC_{50} of 0.55 ± 0.07 μM. RAD001 was only moderately active as a single agent (IC_{50} 15.2 ± 0.8 μM) but, when the cells were treated for 24 h followed by 48 h exposure to sorafenib, the inhibition of cell proliferation was consistently greater than that expected on the basis of simple additive effects. This synergistic interaction progressively increased with increasing drug concentrations, as indicated by the progressive decrease in IC_{50} values from 0.79 to 0.39 (Fig. 4).

In order to test whether the increased cytotoxic effect of sequential treatment with RAD001 and sorafenib was due to the enhanced induction of programmed cell death, the presence of chromatin condensation and DNA fragmentation (common features of apoptosis) was evaluated by means of fluorescence microscopy after staining with propidium iodide

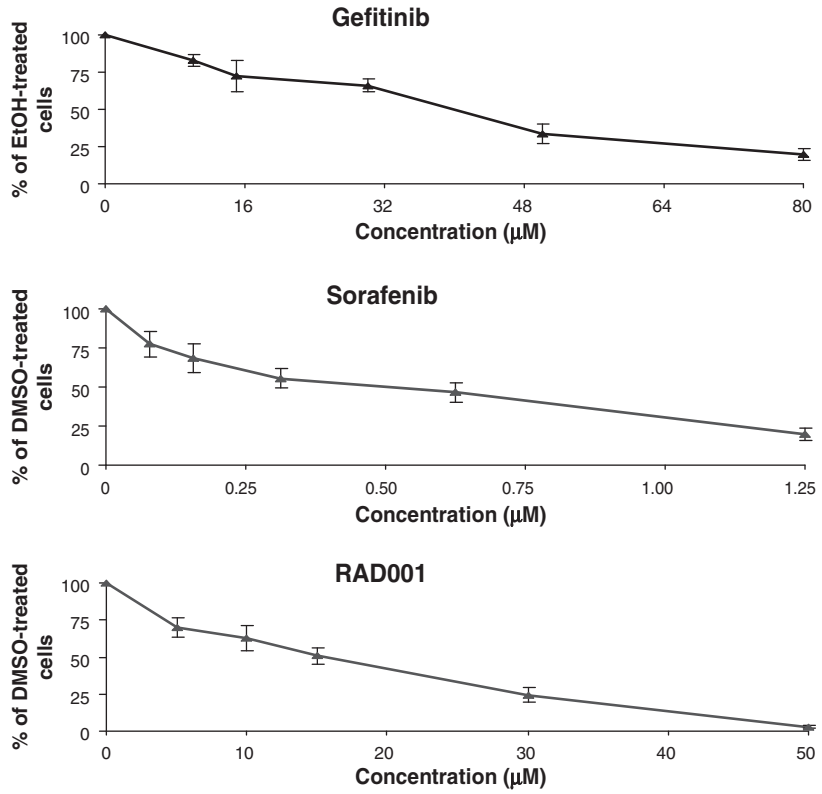

Fig. 3 – Cytotoxic activity of gefitinib, sorafenib and RAD001 in a peritoneal mesothelioma cell line. The cells were cultured for 72 h in the presence of increasing concentrations of gefitinib, sorafenib or RAD001, and cytotoxic activity was assessed by means of an SRB assay. Mean values ± SD of at least three independent experiments.

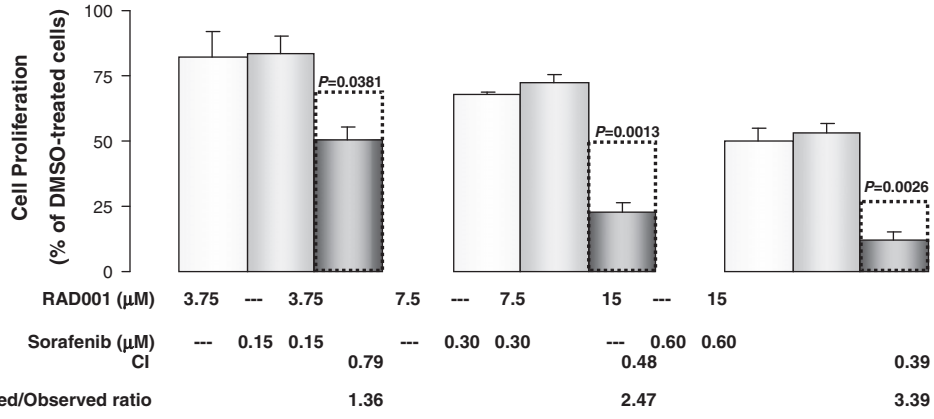

Fig. 4 – Synergistic cytotoxic effect of RAD001 followed by sorafenib. The cells were exposed to RAD001 and sorafenib alone or in sequence at a fixed RAD001:sorafenib dose ratio of 1:25, and the cytotoxic effect was assessed by means of an SRB assay. The dashed lines represent the expected additive effect of the combination, calculated as the product of the effects of the individual drugs. CI was calculated according to Chou and Talalay.[29] Mean values ± SD of at least three independent experiments.

stainining of STO cells treated with the two agents singly and in sequence. In the samples exposed to different RAD001 concentrations, the percentage of cells with an apoptotic nuclear morphology was not significantly different from that observed in the control cells (always <5% of the overall cell population), whereas the samples exposed to 0.6 μM of sorafenib showed a slightly higher percentage (8.6 ± 1.4%) (Fig. 5A). However, the percentage significantly increased in a concentration-dependent manner after sequential treatment with RAD001 and sorafenib, and reached a peak of 23.5 ± 3.6% when the highest concentrations of the drugs were used (Fig. 5A). In line with this observation, at molecular level, an assessment of the *in vitro* hydrolysis of the specific fluorogenic substrate showed that caspase-3 was only slightly

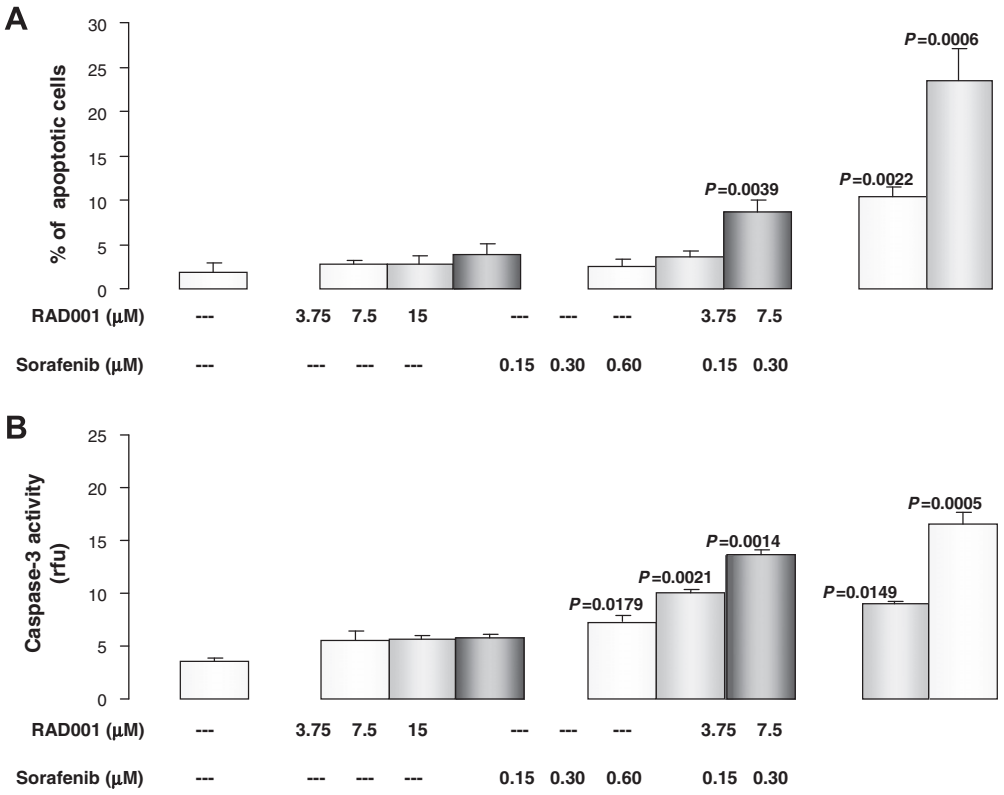

Fig. 5 – Effect of sequential treatment with RAD001 and sorafenib on the induction of apoptosis. The cells were exposed to RAD001 and sorafenib alone or in sequence at a fixed RAD001:sorafenib dose ratio of 1:25. (A) The percentage of cells with an apoptotic nuclear morphology was assessed by means of fluorescence microscopy after staining with propidium iodide. Mean values ± SD of at least three independent experiments. (B) Caspase-3 catalytic activity was determined by means of hydrolysis of the specific fluorogenic substrate. The data are expressed as relative fluorescence units (rfu) and represent the mean values ± SD of at least three independent experiments.

activated in the cells treated with RAD001 alone (Fig. 5B), but significantly activated after sequential exposure to RAD001 and sorafenib (Fig. 5B).

4. Discussion

This study describes the activation profile of RTKs in DMPMs for the first time as assessed using a comprehensive approach based on biochemical and molecular analyses of frozen surgical specimens, complemented by FISH and immunohistochemical analyses of paired fixed material.

We found the expression and phosphorylation of both EGFR and PDGFRB in most of the tumours, and PDGFRA activation in 50%, coupled with the expression of the cognate ligands TGF-α, PDGFB and PDGFA, and the presence of EGFR and PDGFRB heterodimers. Given the absence of any gain in RTK gene copy numbers or activating mutations, these findings suggest an autocrine/paracrine loop coupled with the co-activation of the two RTK families. In particular, we did not find mutation L858R or the other eight novel EGFR mutations (not detailed in terms of type and position) recently found in 31% of DMPMs by means of the SURVEYOR digestion and dHPLC analysis of exons 18–24 spanning the entire EGFR tyrosine kinase domain.[19]

Moreover, analysis of downstream RTK signalling demonstrated the activation/expression of ERK1/2, AKT, mTOR, S6 and 4EBP1 in almost all the DMPMs. Given the absence of *KRAS/BRAF* mutations and *PI3KCA* mutation/amplification, and the inactivation of *PTEN*, this confirms that the phosphorylation of mTOR and its effectors is sustained by activated EGFR and PDGFRB RTKs. We also found that additional RTK-independent mechanisms may be involved in mTOR activation as real-time PCR showed that 54% of the tumours expressed less TSC1 c-DNA than the corresponding non-tumoral tissue, thus suggesting TSC1 loss.

Taken together, these findings support mTOR as a possible therapeutic target to be inhibited by a single agent or, better, by drug combinations including inhibitors of the most activated RTK (Fig. 6). It is worth noting that the lack of significant benefit using EGFR tyrosine kinase inhibitors[31,32] and a single agent Gleevec (a PDGFRB and PDGFRA inhibitor)[33,34] in pleural mesothelioma was observed in patients selected on the basis of an immunohistochemical RTK profile restricted to receptor expression (EGFR; PDGFRB)[16–18] in fixed samples.

In the light of evidence that not only RTK mutation and gene amplification, but also autocrine/paracrine loop activation with or without intra- or inter-family RTK cross-talk, may contribute to the clinical response to targeted therapies,[35] we evaluated the possible antiproliferative effects of EGFR and mTOR inhibitors using the STO human peritoneal mesothelioma cell line established in our laboratory[13] and bearing activated EGFR, AKT, ERK1/2, mTOR, S6 and 4EBP1.

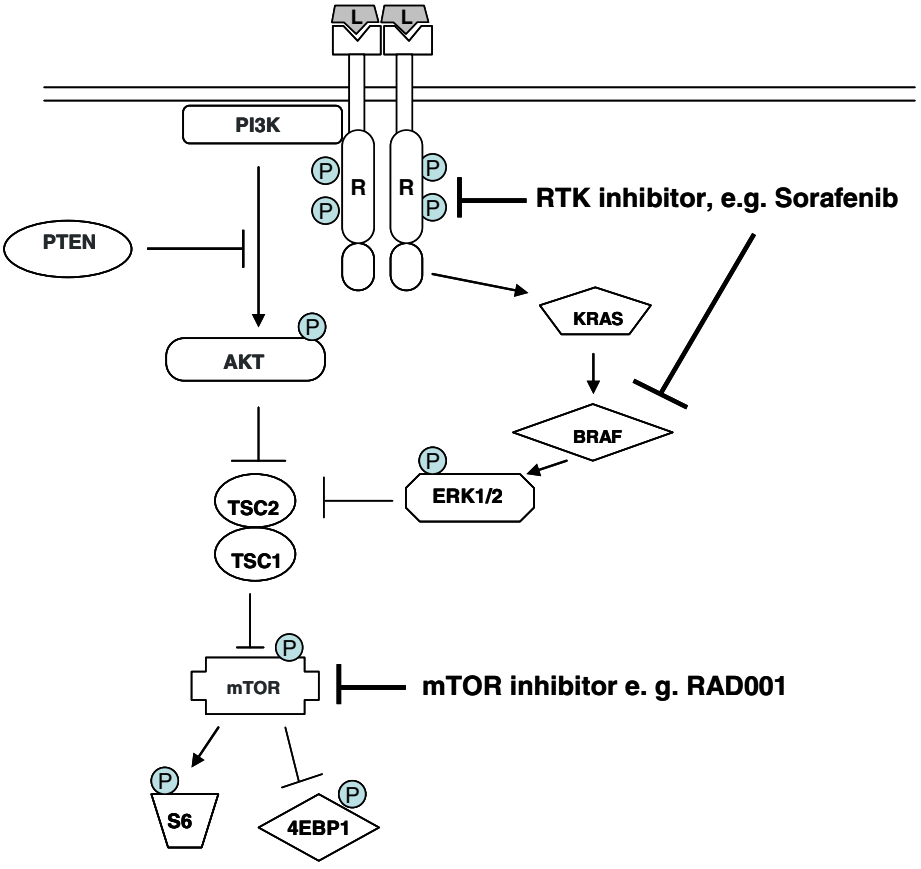

Fig. 6 – RTK pathway. Receptor tyrosine kinase and mTOR may be potential therapeutic targets in DMPM. L, ligand; R, receptor tyrosine kinase; P, phosphorylation.

Unexpectedly, the antiproliferative effect of gefitinib could only be appreciated at very high drug concentrations, and analysis of the downstream RTK effectors showed that, unlike the surgical DMPM specimens, this cell line harbours a KRAS mutation that is known to induce resistance to anti-EGFR treatment.[27] However, a consistently increased cytotoxic effect was observed in after sequential treatment with RAD001 and sorafenib, with evidence of a significant enhancement in apoptotic rate and caspase-3 activity. These results were different from those originally hypothesised but, in line with the KRAS-mediated activation profile of the STO cell line, they confirmed the effectiveness of RTK inhibitors when they are critically selected on the basis of tumoural signalling deregulation and/or closely match the tumoural RTK deregulation profile.

Although EGFR, PDGFRB and mTOR appear to be promising for the treatment of DMPMs, it is necessary to consider the possibility that DMPMs are not exclusively driven by EGFR and PDGFRB activation, and that additional escape mechanisms co-exist. Together with M-CSF-R, which belongs to the same family as PDGFRB, other RTKs warrant further investigation, such as the IGF-1R and insulin receptors that were activated in the four DMPMs we analysed using the phospho-proteome profiler array kit. The same is true of MET, whose activation in pleural mesothelioma cell lines has been extensively reported,[36] but was not found in the two DMPM cases we randomly analysed (data not shown). In addition to RTK, p16 status may also be relevant as it is frequently down-regulated in DMPM[5] and 60% of our cases were devoid of p16 at immunohistochemistry without any evidence of gene loss. Finally, our finding of TSC1 c-DNA levels merits further investigation by means of mutational and microsatellite analyses.

In conclusion, the results of this study highlight the existence of the ligand-dependent activation of, and cross-talk between EGFR and PDGFRB, and a connection between them and the downstream pathway of mTOR, a key regulator of cell growth as a result of its regulation of protein synthesis through its S6 and 4EBP1 effectors. Apart from the possible consequent negative feedback loop of PI3K/AKT[37] and the MAP pathway,[38] these findings support the role of combined treatment with RTK and mTOR inhibitors in DMPM (Fig. 6).

Conflict of interest statement

None declared.

Acknowledgements

The authors wish to greatly acknowledge the financial support received from Istituto Superiore Sanita' and Associazione Italiana per la Ricerca sul Cancro.

REFERENCES

1. Deraco M, Bartlett D, Kusamura S, Baratti D. Consensus statement on peritoneal mesothelioma. *J Surg Oncol* 2008;**98**:268–72.
2. Yan TD, Deraco M, Baratti D, et al. Cytoreductive surgery and hyperthermic intraperitoneal chemotherapy for malignant peritoneal mesothelioma: multi-institutional experience. *J Clin Oncol* 2009;**27**:6237–42.
3. Carteni G, Manegold C, Garcia GM, Siena S, et al. Malignant peritoneal mesothelioma – results from the International Expanded Access Program using pemetrexed alone or in combination with a platinum agent. *Lung Cancer* 2009;**64**:211–8.
4. Baratti D, Kusamura S, Cabras AD, et al. Diffuse malignant peritoneal mesothelioma: Failure analysis following cytoreduction and hyperthermic intraperitoneal chemotherapy (HIPEC). *Ann Surg Oncol* 2009;**16**: 463–72.
5. Nonaka D, Kusamura S, Baratti D, et al. Diffuse malignant mesothelioma of the peritoneum: a clinicopathological study of 35 patients treated locoregionally at a single institution. *Cancer* 2005;**104**:2181–8.
6. Chiosea S, Krasinskas A, Cagle PT, et al. Diagnostic importance of 9p21 homozygous deletion in malignant mesotheliomas. *Mod Pathol* 2008;**21**:742–7.
7. Illei PB, Rusch VW, Zakowski MF. And Ladanyi M Homozygous deletion of CDKN2A and codeletion of the methylthioadenosine phosphorylase gene in the majority of pleural mesotheliomas. *Clin Cancer Res* 2003;**9**:2108–13.
8. Deraco M, Nonaka D, Baratti D, et al. Prognostic analysis of clinicopathologic factors in 49 patients with diffuse malignant peritoneal mesothelioma treated with cytoreductive surgery and intraperitoneal hyperthermic perfusion. *Ann Surg Oncol* 2006;**13**:229–37.
9. Trupiano JK, Geisinger KR, Willingham MC, et al. Diffuse malignant mesothelioma of the peritoneum and pleura, analysis of markers. *Mod Pathol* 2004;**17**:476–81.
10. Butnor KJ, Burchette JL, Sporn TA, Hammar SP, Roggli VL. The spectrum of Kit (CD117) immunoreactivity in lung and pleural tumors: a study of 96 cases using a single-source antibody with a review of the literature. *Arch Pathol Lab Med* 2004;**128**:538–43.
11. Borczuk AC, Taub RN, Hesdorffer M, et al. P16 loss and mitotic activity predict poor survival in patients with peritoneal malignant mesothelioma. *Clin Cancer Res* 2005;**11**:3303–8.
12. Villa R, Daidone MG, Motta R, et al. Multiple mechanisms of telomere maintenance exist and differentially affect clinical outcome in diffuse malignant peritoneal mesothelioma. *Clin Cancer Res* 2008;**14**:4134–40.
13. Zaffaroni N, Costa A, Pennati M, et al. Survivin is highly expressed and promotes cell survival in malignant peritoneal mesothelioma. *Cell Oncol* 2007;**29**:453–66.
14. Giaccone G, Zatloukal P, Roubec J, et al. Multicenter phase II trial of YM155, a small-molecule suppressor of survivin, in patients with advanced, refractory, non-small-cell lung cancer. *J Clin Oncol* 2009;**27**:4481–6.
15. Borczuk AC, Cappellini GCA, Kim HK, et al. Molecular profiling of malignant peritoneal mesothelioma identifies the ubiquitin-proteasome pathway as a therapeutic target in poor prognosis tumors. *Oncogene* 2007;**26**:610–7.
16. Kothmaier H, Quehenberger F, Halbwedl I, et al. EGFR and PDGFR differentially promote growth in malignant epithelioid mesothelioma of short and long term survivors. *Thorax* 2008;**63**:345–51.
17. Langerak AW, De Laat PA, Van Der Linden-Van Beurden CA. Et al.Expression of platelet-derived growth factor (PDGF) and PDGF receptors in human malignant mesothelioma *in vitro* and *in vivo*. *J Pathol* 1996;**178**:151–60.
18. Roberts F, Harper CM, Downie I, Burnett RA. Immunohistochemical analysis still has a limited role in the diagnosis of malignant mesothelioma. A study of thirteen antibodies. *Am J Clin Pathol* 2001;**116**:253–62.
19. Foster JM, Gatalica Z, Lilleberg S, Haynatzki G, Loggie BW. Novel and existing mutations in the tyrosine kinase domain of the epidermal growth factor receptor are predictors of optimal resectability in malignant peritoneal mesothelioma. *Ann Surg Oncol* 2009;**16**:152–8.
20. Tamborini E, Bonadiman L, Greco A, et al. Expression of ligand-activated KIT and platelet-derived growth factor receptor beta tyrosine kinase receptors in synovial sarcoma. *Clin Cancer Res* 2004;**10**:938–43.
21. Perrone F, Da Riva L, Orsenigo M, et al. PDGFRA, PDGFRB, EGFR, and downstream signalling activation in malignant peripheral nerve sheath tumor. *Neuro Oncol* 2009;**11**:725–36.
22. Lagonigro MS, Tamborini E, Negri T, et al. PDGFRalpha, PDGFRbeta and KIT expression/activation in conventional chondrosarcoma. *J Pathol* 2006;**208**:615–23.
23. Stacchiotti S, Tamborini E, Marrari A, et al. Response to sunitinib malate in advanced alveolar soft part sarcoma. *Clin Cancer Res* 2009;**15**:1096–104.
24. Perrone F, Suardi S, Pastore E, et al. Molecular and cytogenetic subgroups of oropharyngeal squamous cell carcinoma. *Clin Cancer Res* 2006;**12**:6643–51.
25. Tamborini E, Casieri P, Miselli F, et al. Analysis of potential receptor tyrosine kinase targets in intimal and mural sarcomas. *J Pathos* 2007;**212**:227–35.
26. Tamborini E, Miselli F, Negri T, et al. Molecular and biochemical analyses of platelet-derived growth factor receptor (PDGFR) B, PDGFRA, and KIT receptors in chordomas. *Clin Cancer Res* 2006;**12**:6920–8.
27. Perrone F, Lampis A, Orsenigo M, et al. PI3KCA/PTEN deregulation contributes to impaired responses to cetuximab in metastatic colorectal cancer patients. *Ann Oncol* 2009;**20**:84–90.
28. Skehan P, Storeng R, Scudiero, et al. New colorimetric cytotoxicity assay for anticancer-drug screening. *J Natl Cancer Inst* 1990;**82**:1107–12.
29. Chou TC, Talalay P. Quantitative analysis of dose-effect relationships: the combined effects of multiple drugs or enzyme inhibitors. *Adv Enzyme Regul* 1984;**22**:27–55.
30. Porta C, Paglino C, Imarisio I, Ferraris E. Sorafenib tosylate in advanced kidney cancer: past, present and future. *Anticancer Drugs* 2009;**20**:409–15.
31. Govindan R, Kratzke RA, Herndon 2nd JE. Gefitinib in patients with malignant mesothelioma: a phase II study by the cancer and leukemia group B. *Clin Cancer Res* 2005;**11**:2300–4.
32. Garland LL, Rankin C, Gandara DR, et al. Phase II study of erlotinib in patients with malignant pleural mesothelioma: a southwest oncology group study. *Clin Oncol* 2007;**25**:2406–13.
33. Porta C, Mutti L, Tassi G. Negative results of an Italian Group for Mesothelioma (G.I.Me.) pilot study of single-agent imatinib mesylate in malignant pleural mesothelioma. *Cancer Chemother Pharmacol* 2007;**59**:149–50.
34. Mathy A, Baas P, Dalesio O, van Zandwijk N. Limited efficacy of imatinib mesylate in malignant mesothelioma: a phase II trial. *Lung Cancer* 2005;**50**:83–6.
35. Pierotti MA, Negri T, Tamborini E, et al. Targeted therapies: the rare cancer paradigm. *Mol Oncol* 2010;**4**: 19–37.

36. Kawaguchi K, Murakami H, Taniguchi T, et al. Combined inhibition of MET and EGFR suppresses proliferation of malignant mesothelioma cells. *Carcinogenesis* 2009;**30**:1097–105.
37. Manning BD, Logsdon MN, Lipovsky AI, et al. Feedback inhibition of Akt signaling limits the growth of tumors lacking Tsc2. *Genes Dev* 2005;**19**:1773–8.
38. Carracedo A, Ma L, Teruya-Feldstein J, et al. Inhibition of mTORC1 leads to MAPK pathway activation through a PI3K-dependent feedback loop in human cancer. *J Clin Invest* 2008;**118**:3065–74.